Effectiveness of Plants and Vegetation in Erosion Control and Restoration

Sandercock, P.; Hooke, J.; De Baets, S.; Poesen, J.; Meerkerk, A.; van Wesemael, B.; Cammeraat, L.H.

DOI
10.1007/978-3-319-44451-2_4

Publication date
2017

Document Version
Final published version

Published in
Combating Desertification and Land Degradation

Chapter 4
Effectiveness of Plants and Vegetation in Erosion Control and Restoration

Peter Sandercock, Janet Hooke, Sarah De Baets, Jean Poesen, André Meerkerk, Bas van Wesemael, and L.H. Cammeraat

Abstract In this chapter the approaches and methods used to measure plant effectiveness in reducing runoff and erosion are explained and results presented for each of the major land units, hillslopes and channels. Evaluations of the properties of plants required are made to inform plant selection for different sites. For use of cover crops in orchards it is important to assess whether the cover crops would have an effect on orchard tree productivity, whilst also reducing soil erosion. A climatic threshold for their use was identified. Soil moisture measurements from different treatment areas and water balance and runoff modelling exercises showed where use of such crops could be beneficial. Extent of vegetation growth on abandoned lands was shown to have a marked effect on runoff, water repellency and soil crusts. Various root parameters were measured on a range of plants and their relation to soil detachment calculated. Differences in root architecture and in orientation of rows of plants were tested. Plant stem density, stem bending and trapping efficiency effects

P. Sandercock (✉)
Jacobs, 80A Mitchell St, PO Box 952, Bendigo, VIC, Australia
e-mail: Peter.Sandercock@jacobs.com

J. Hooke
Department of Geography and Planning, School of Environmental Sciences,
University of Liverpool, Roxby Building, L69 7ZT Liverpool, UK

S. De Baets
College of Life and Environmental Sciences, Department of Geography,
University of Exeter, Rennes Drive, EX4 4RJ Exeter, UK

J. Poesen
Division of Geography and Tourism, Department of Earth and Environmental Sciences,
KU Leuven, Celestijnenlaan 200E, 3001 Heverlee, Belgium

A. Meerkerk • B. van Wesemael
Earth and Life Institute, Université catholique de Louvain (UCL),
Place Louis Pasteur 3, 1348 Louvain-la-Neuve, Belgium

L.H. Cammeraat
Instituut voor Biodiversiteit en Ecosysteem Dynamica (IBED)
Earth Surface Science, Universiteit van Amsterdam, Science Park 904,
1098 XH Amsterdam, The Netherlands

J. Hooke, P. Sandercock, *Combating Desertification and Land Degradation*,
SpringerBriefs in Environmental Science, DOI 10.1007/978-3-319-44451-2_4

were also assessed experimentally and plant species growing in the Mediterranean study area were grouped according to their erosion control potential. The effects of vegetation and various plant species on roughness, flow hydraulics and sediment trapping in channels were assessed by field measurements and modelling and their resilience to high flow evaluated from observed flood impacts.

Keywords Erosion control effectiveness • Cover crops • Crop water balance • Plant root properties • Vegetated channel roughness • Flood impacts on vegetation

4.1 Introduction

Understanding the effect that plants and vegetation have on processes is critical to assessing their effectiveness in prevention of erosion and selection for use in the stabilisation of degraded lands. In this chapter the approaches and methods used to measure plant effectiveness in reducing runoff and erosion are explained. Results of each are exemplified. Evaluations of the properties of plants required are made to inform plant selection for different sites. These aspects are discussed and exemplified for each of the major land units then hillslopes and channels.

4.2 Land Units

4.2.1 Cover Crops

The main issue in relation to assessment of effectiveness of cover crops is not only its ability to reduce erosion but also to determine whether it affects productivity of the main crop, through reduction of water availability. The effectiveness of cover crops can be assessed at the field scale using a number of different approaches. Three approaches were taken within the project: (1) calculation of climatic thresholds, (2) soil moisture measurements from different treatment areas (i.e. areas with and without cover crops), and (3) water balance and runoff modelling exercises to investigate the availability of water under different climate and soil conditions.

4.2.1.1 Identification of a Climatic Threshold

Whereas climate determines the upper limit of available water, an attempt was undertaken to identify climatic thresholds for cover crops in olive orchards. This study was based on the relation between tree density, projected canopy cover and climate (Meerkerk et al. 2008). As a climatic indicator the ratio between annual precipitation and the reference evapotranspiration was used. In the literature this ratio is referred to as the aridity index (Lioubimtseva et al. 2005; UNEP 1997) or humidity index (Yin et al. 2005). The term humidity index (*HI*) is used here because this index increases with increasing humidity. It can be noted that the semi-arid climatic zone is defined by $0.2 <= HI < 0.5$ (UNEP 1997). During the project a considerable amount of data on olive orchards was gathered, both from fieldwork in Southeast Spain and from colleagues and literature sources throughout the Mediterranean. For each observation, *HI* was calculated using data from the A-Team climate database (Mitchell et al. 2002). Evapotranspiration was estimated with the Hargreaves equation, using monthly input data (for details see Allen et al. 1998).

The results produced a significant correlation between tree density or canopy cover and *HI*, which is nevertheless rather weak (Meerkerk et al. 2008). It appears that for locations with $HI > 0.6$, the growth of the olive trees is no longer limited by water availability and there is a surplus of water that could be used to grow cover crops. Below the threshold, the use of cover crops must be restricted in space and time in order to avoid competition for water. This threshold coincides with the crop factor, K_c. Probably, for other perennial crops the K_c can be used as a climatic threshold as well.

4.2.1.2 Experimental Field Study

Soil moisture measurements were set up in an olive orchard west of Sevilla (UTM 29S 745565E 4136755 N) (in collaboration with colleagues from CSIC Córdoba) (Fig. 4.1). The experiment consists of the comparison of two treatments: (1) no-turning tillage (3–5 times per year) and (2) a grass cover in the traffic lane that is killed in spring with herbicides. The soil moisture is measured at depths of 7, 15, 21 and 45 cm using theta probes. Two sensors were installed per treatment at 45 cm. Only preliminary results were obtained within the period of the RECONDES project and are not discussed here.

4.2.1.3 Water Balance and Runoff Modelling

The aim of the water balance modelling exercise was to compare the effect of different climatic and soil conditions on water availability in rainfed cropping systems. It serves to improve our knowledge on the water availability for cover crops and competition with the main crop (Meerkerk et al. 2008).

For the almond orchards studied in Murcia, a two-layer approach is used in order to distinguish evaporation losses from the plough layer and the water in the underlying soil, which is available for transpiration by the trees. This conceptual model builds on two assumptions. The first assumption is that no drainage occurs below the rooting zone of the almond trees. This is realistic under semi-arid conditions, since the amount of rain from individual rainfall events is small. For example, in the Cárcavo target area, a 35-year record of weather data reveals that the rainfall exceeds

Fig. 4.1 The experimental site west of Sevilla. Upper: no-turning tillage. Lower: cover crop treatment (Meerkerk et al. 2008)

30 mm only during 3 % of the rainy days. Furthermore, the roots of full grown trees may extend up to 14 m from the trunk and a few meters deep if the soil is deep enough (Micke 1996). This means that although the trees are typically spaced about 7 m apart, their roots can potentially extract water from the complete orchard surface, limiting drainage. The second assumption of the model is that no almond roots occur in the 15 cm deep plough layer; the soil is kept bare during the major part of the year by frequent tillage.

In order to verify the validity of these assumptions, a survey was done of the presence of roots in the upper 25 cm of the soil in an almond orchard in Cárcavo. In total 42 root observations were done at distances of 0.5–4 m from the trunks, examining vertical 10 by 10 cm squares of soil at a depth of 15 and 25 cm. In 11 pits (25 %) no roots were encountered at all, and in just 2 pits (5 %) there were more than ten roots per 100 cm^2 window. Roots with a diameter beyond 1 mm were observed in seven pits (17 %), of which six pits had a single root of that size and one pit had two. Sometimes the roots could be related to weed remnants, supporting the conclusion that the presence of tree roots in the plough layer is quite restricted.

Modelling was used to test the hypothesis that the evaporation loss from the plough layer (E_p) can be used without competition with the trees by a shallow rooting cover crop (Meerkerk et al. 2008). In other words, the deep rooting almond crop and shallow rooting cover crop derive their water from different parts of the soil. The water balance of the plough layer can be written as:

$$E_p = P - D - \Delta S - Q_{off} + Q_{on} \tag{4.1}$$

where E_p is evaporation loss from the plough layer (mm), P is precipitation (mm), D is drainage below the plough layer(mm), ΔS is change in soil moisture storage for a given time interval (mm), Q_{off} is runoff (mm), Q_{on} is run-on (mm).

Two soil types were selected for a simulation exercise, consisting of a silt loam soil on marl and a stony soil on slate and phyllites. The contrasting properties of these soils allow us to obtain a broad picture of the water balance and evaporation loss from the plough layer in Murcia. The BUDGET model (Raes et al. 2006), is able to simulate the water balance of both soil types quite well. BUDGET was calibrated by means of a lysimeter experiment which included two soil columns per soil type with a diameter of 30 cm. For the calibration, three parameters of the model needed to be adjusted for each soil column: depth of evaporation, field capacity or wilting point and tau, which determines the rate of drainage within the soil profile. The simulation errors of the calibrated model were smaller than 11 mm for all components of the water balance and the root mean square error in soil moisture was below 4.6 %. Runoff was estimated based on the initial abstraction before runoff and the saturated hydraulic conductivity of the soil. An empirical relation was used that estimates the maximum 10-min rainfall intensity from hourly rainfall records ($R^2 = 0.66$; $n = 118$), as well as the intensity of the rain that falls during the remaining 50 min.

Model runs were executed with hourly weather data measured by UvA at a field site 16 km northwest of Lorca (Alqueria station). Next to a year with average rainfall (287 mm), a dry (169 mm) and wet (429 mm) year were selected, having a return period of approximately 7 years. This range in annual rainfall should be considered in the design and management of the rainfed orchards and cover crops, in order to avoid an unsustainable tree mortality rate in dry years.

A part of the model input data was derived from field measurements that were carried out in Cárcavo in January and September 2005. The dry bulk density of the top soil ranged from 1000 to 1200 kg/m^3. The hydraulic conductivity of the top soil (K_{sat}) was determined by rainfall simulation on freshly ploughed soils and soils with a structural crust. The freshly ploughed soils developed a structural crust after just one rainfall event. The observed K_{sat} values ranged from 18 to 31 mm/h. The average for non-crusted soil was 29 mm/h and for crusted soil 23 mm/h. Another input was the soil albedo, which was measured during fieldwork in January 2006.

The results of the simulation study show that the evaporation loss is 52–112 mm higher on the marl soil for the 'wet' and 'average' year compared to the stony soil. This difference is directly related to the deeper infiltration of the rain on the stony soils. In the 'average' and 'dry' year, there is no drainage below 33 cm on the marl, due to the small size of the rains (<=41 mm) and low antecedent soil moisture. Another difference is the occurrence of runoff on the marl soils, which increases the

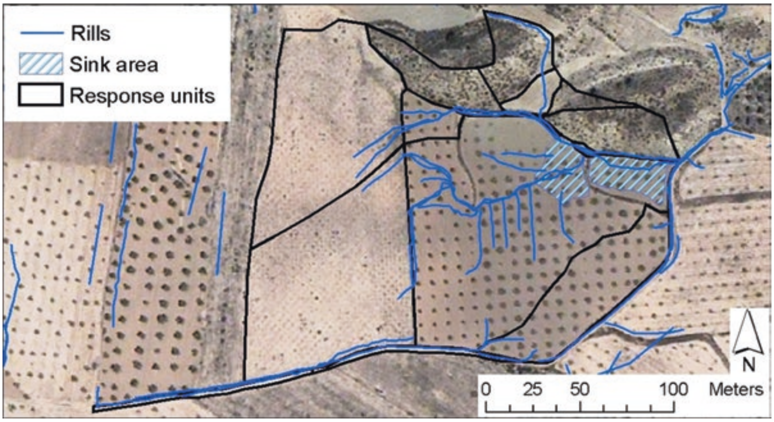

Fig. 4.2 Pathways of runoff and hydrological response units in Cárcavo (After Meerkerk et al. 2008)

spatial variability in soil moisture within the orchard. For the simulation years, there were 1–7 runoff events per year. Although runoff coefficients are low (1–5 %), runoff can still make an important difference in the spatial variability of soil moisture, tree growth and water availability for cover crops.

The evaporation loss from a 15-cm plough layer during autumn and winter, ranges from 100 to 155 mm, and varies little between the different soils. The evapotranspiration of a shallow rooting cover crop would use a similar amount of water. This means that there are opportunities for applying cover crops without a negative effect on the growth and yield of the tree crop. The amounts of runoff produced on the marl soils are relatively small.

This was studied in more detail for one almond field in Cárcavo, in order to determine whether the infiltration of runoff in depressions and thalwegs makes a significant difference in terms of water availability and vegetation growth (Fig. 4.2). The model results show that on an annual basis, the infiltration in the sink area within the field is 95–385 mm higher compared to the slope position (Table 4.1). An analysis of the tree trunk diameter of the trees in the sink area shows that the extra infiltration has a positive effect on tree vigour. The trunk basal area was 12 % larger at the age of 4 years ($p < 0.03$). This result shows that specific landscape positions may provide increased water availability and a higher potential for the growth of cover crops without competition with the tree crop in dry conditions.

4.2.2 Semi-Natural, Abandoned and Reforested Lands

Field monitoring of occurrence of runoff in different locations made it clear that vegetation has a significant effect on the pathways of water and sediment. The infiltration under vegetation patches is much higher and deeper, compared to bare

Table 4.1 Water balance of a 15 cm plough layer at different topographical positions. The reference refers to a position where run-on and run-off are equal (After Meerkerk et al. 2008)

	Year	Qon	I	Qoff	D	E	dS
Slope position:	Dry	–	166	3	0	166	0
	Average	–	285	2	39	245	1
	Wet	–	416	13	117	298	1
Sink position:	Dry	92	261	11	84	177	0
	Average	61	348	0	102	245	1
	Wet	372	801	189	476	324	1
Reference:	Dry	–	169	–	0	169	0
	Average	–	287	–	41	245	1
	Wet	–	429	–	130	299	0

Table 4.2 Reaction of runoff indicators after nine rainfall events

ID	Location	Vegetation cover (%)	Runoff occurrence
1	On 70 % south slope	50	4
2	At end of large gully	80	4.5
3	On 50 % south slope	15	6
4	At end of large gully	40	6.5
5	At end of small low gully in terrace wall	70	1.5
6	Before gully head	20	4.5
7	At end of large gully	30	7
8	At 45 % north slope	30	7
9	At 30 % north slope	90	3
10	Before gully head	55	3
11	Before gully head in terrace wall	40	6
12	At end of gully in the terrace wall	95	1

patches and also the temperature under vegetation is more regulated and the daily variation is less. The infiltration and sedimentation behind vegetation is also clear from the runoff indicators (Table 4.2). The occurrence of runoff for similar locations is more frequent when the vegetation cover is lower, e.g. runoff indicator 1 versus 3 or runoff indicator 2 versus 7. Threshold for runoff occurrence can be calculated by comparing the occurrence of runoff with the amount and intensity of rainfall.

Water repellency is associated with organic matter and vegetation. It was measured in the field using drop tests and time for penetration of water. Figure 4.3 shows the relationship between soil moisture, plant species and water repellency for *Rosmarinus* and *Anthyllis*. *Stipa* litter was found to be far less water repellent (not shown in figure). Figure 4.4 shows the relationship between accumulated organic matter and water repellency for the studied vegetation. For restoration purposes it should be taken into account that soils and accumulated organic matter with higher water repellency will increase the amount of local runoff, and may generate unwanted connectivity in the hydrological system. This may especially be a problem after prolonged dry periods with sudden high intensity rainfall.

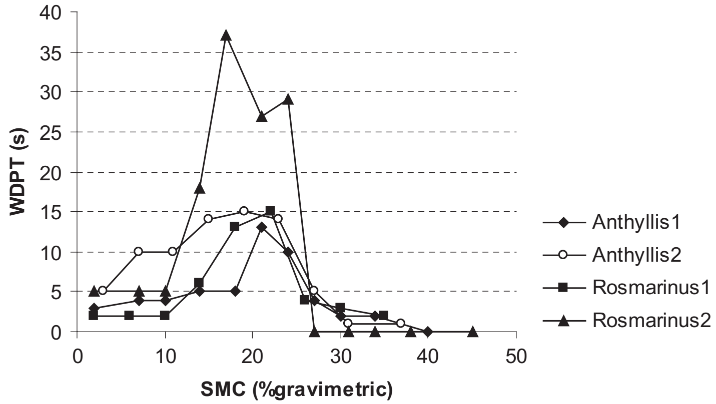

Fig. 4.3 Distribution of crust water repellency for two plant species in a wetting range. *SMC* soil moisture content, *WDPT* water drop penetration time. Each data point is the average WDPT of five droplets (Verheijen and Cammeraat 2007). Copyright © 2007 John Wiley & Sons, Ltd

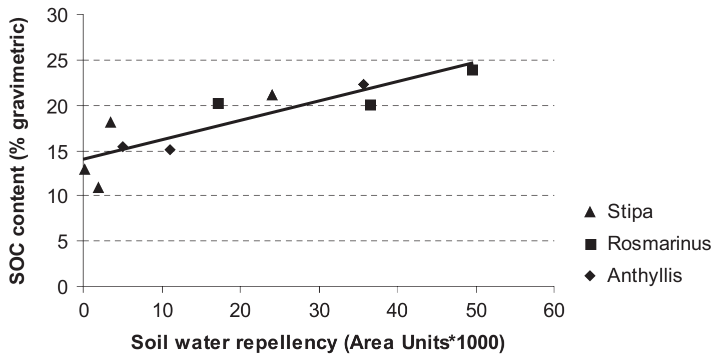

Fig. 4.4 The correlation of water repellency with SOC content of the mulch samples; r2 = 0.74 and p = 0.01. Insufficient mulch sample for SOC analysis was available for one Stipa, two Rosmarinus and two Anthyllis plants (Verheijen and Cammeraat 2007). Copyright © 2007 John Wiley & Sons, Ltd

The effect of vegetation on *soil crusts* was assessed by sampling thin sections of crusts on marls and calcretes with low organic carbon contents from fields that were abandoned and from semi-natural vegetation. The soil crusts were studied with respect to: (a) effects of material, (b) effects of geomorphological processes and (c) interaction with plants. The development of soil crusts was also studied in the laboratory under simulated rainfall.

The results from the thin section analysis showed that the crust properties are linked to their position in relation to plants and that these can explain hydrological behaviour. Figure 4.5 shows a clear contrast of soil surface properties up and down slope of a *Stipa tenacissima* tussock. The left photo shows a sedimentation crust with many vesicles and some organic matter accumulation, whereas the right

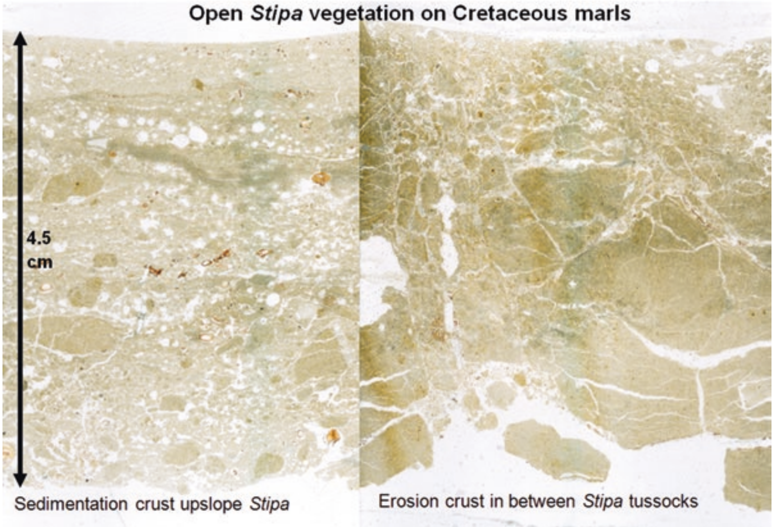

Fig. 4.5 Comparison between a sedimentation crust upslope a *Stipa tenacissima* tussock, and an erosion crust down slope a *Stipa* tenacissima tussock

photograph shows the badly developed soil surface with the marl substratum very close to the surface, as soil surface material has been washed away. This consequently has very important repercussions for runoff generation at the fine scale for areas such as described in Fig. 2.2 (Chap. 2). Figure 4.6 shows a multiple deposition crust under a fermentation layer on a reforestation terrace in Cretaceous marls. It also shows the change of runoff and sedimentation regime after the growth of the vegetation as the original crust prior to planting also is visible. This shows that overland flow frequently occurs, and that it is infiltrating for most of the events occurring. However, the terrace rim also showed serious signs of erosion from high magnitude events. Furthermore, crust evolution simulation revealed that sieving crusts, as present in the study area, can be created within 4 years. This was concluded from thin sections made from different stages of development after rainfall simulations in the laboratory and from sampled field sieving crusts that had developed after 40 years of abandonment in the same material.

4.3 Role of Plants in Reducing Concentrated Flow Erosion Rates

Within the RECONDES project detailed investigations were carried out into the effects of roots of Mediterranean plant species on soil resistance to concentrated flow erosion. Roots are the hidden half of plants that play a key role in rill-gully erosion and shallow mass movements (Vannoppen et al. 2015). Research methods

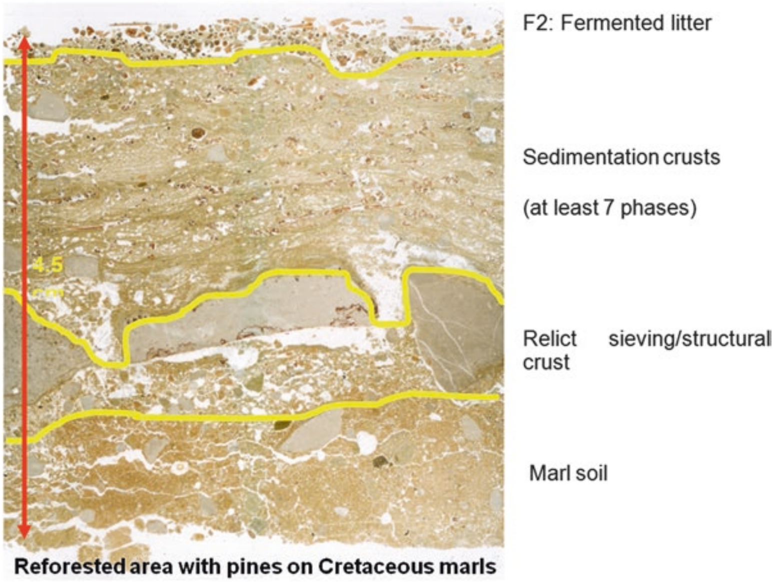

Fig. 4.6 Multiple sedimentation crusts on a reforestation terrace planted with *Pinus halepensis*

included laboratory flume experiments, fieldwork, and laboratory tensile and bending strength measurements. Detailed methods and results have been published in a series of papers (see papers by De Baets et al.). They are summarised briefly here to illustrate the approaches.

4.3.1 Laboratory and Flume Experiments

The overall objective was to gain more insight into the influence of root architecture, soil and flow characteristics on the effects of plant roots in increasing the erosion resistance of topsoils during concentrated flow. More specific objectives were:

1. To assess the impact of root architecture (tap root systems vs. fine-branched root systems) on the erosion-reducing potential of roots during concentrated flow,
2. To assess the impact of soil texture (sandy loam vs. silt loam) on the potential of roots to increase the resistance of the topsoil against concentrated flow erosion,
3. To assess the impact of soil moisture content (wet vs. dry topsoil samples) on the erosion-reducing potential of roots during concentrated flow,
4. To assess the impact of flow shear stress on the erosion-reducing potential of roots during concentrated flow.
5. To determine the effect of the spatial organisation of plants on the erosion-reducing potential of roots during concentrated flow.

Six field plots (length = 1.19 m, width = 0.97 m, and soil depth = 0.15 m for each) were established at Leuven University Campus on a sandy loam soil (8 % clay/< 2 μm, 36 % silt/50–2 μm and 56 % sand/50 μm–2 mm in year 1). In year 2 six plots were established at the same place on a silt loam soil (9 % clay/< 2 μm, 70 % silt/2–50 μm and 21 % sand/50 μm–2 mm). Treatments were: (1) bare; (2) grass (simulating fine-branched roots, low and high density drilling), and; (3) carrots (simulating taproots, low and high density drilling). For the assessment of the effect of spatial organisation of plants, treatments were: (1) bare; (2) grass randomly sown, and; (3) grass sown in rows with an inter-row distance of 5 cm. Differing variables between the samples tested are type of species, flow shear stress level, soil type and soil moisture conditions.

Laboratory experiments simulating concentrated flow were conducted with a flume similar to the one used by Poesen et al. (1999) (Fig. 4.7; length = 2 m, width = 0.098 m). The slope of the flume surface could be varied and clear tap water flow could be simulated at a known constant discharge. The erosion parameters calculated included relative soil detachment rate (*RSD*). *RSD* was calculated as the ratio between absolute soil detachment rate (*ASD*) for the root-permeated soil samples and the *ASD* for the bare topsoil samples, tested at the same time. *ASD* rate for each sample was calculated using the following equation:

$$ASD = (SC * Q) / A \tag{4.2}$$

where *SC* is sediment concentration (kg l^{-1}), *Q* is flow discharge (l s^{-1}) and *A* is area of soil sample surface (m^2).

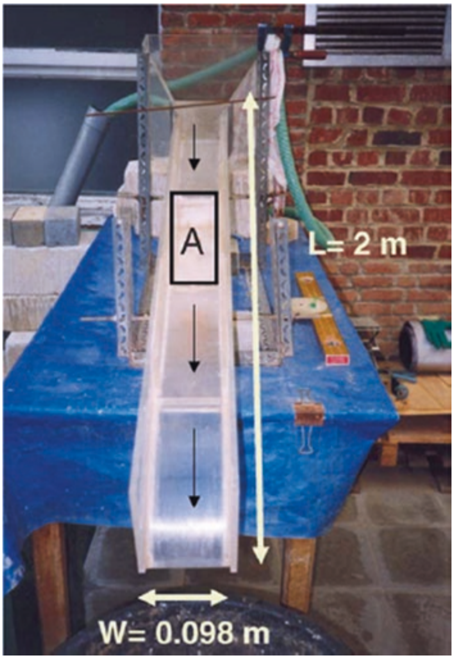

Fig. 4.7 Hydraulic flume at KU Leuven used to measure detachment rates from root permeated topsoil samples. A is the test section (length = 38.8 cm, depth = 8.8 cm, width = 9 cm). *Arrows* indicate concentrated flow direction

Assessed root parameters were root density (*RD*), root length density (*RLD*) and root diameter (*D*) because of their relevance for evaluating the effects of roots on erosion processes (Gyssels and Poesen 2003; Li et al. 1991; Mamo and Bubenzer 2001a, 2001b). *RD* (kg m^{-3}) in this study is expressed by the dry mass of the living roots divided by the volume of the root-permeated soil sample:

$$RD = \frac{M_D}{V} \tag{4.3}$$

where M_D is dry living root mass (kg) and V is volume of the sample box (m^3).

RLD is the total length of the roots divided by the volume of the root-permeated soil sample (Smit et al. 2000):

$$RLD = \frac{L_R}{V} \tag{4.4}$$

where L_R is length of the living roots (km).

In this study mean root diameter (*D*, mm) for each sample was also assessed to investigate the suitability of this root parameter for improving the prediction of the erosion-reducing effect of roots (De Baets et al. 2006, 2007a).

4.3.1.1 Results

Correlation analysis indicates that *RD*, *RLD* and *D* are well correlated with lnR*SD*. The best model, establishing single non-linear regression equations between all influencing variables and *RSD (relative soil detachment rate)*, was obtained with *RD* ($R^2 = 0.59$). Our experimental results show that roots can reduce erosion rates to very low values (for very low *RD*), in contrast to what was previously thought. The results of the laboratory experiments do confirm that the erosion-reducing effect of roots is dependent on root architectural properties. Root diameter (*D*) does influence the erosion-reducing potential of roots during concentrated flow. *RD* and *D* explain the observed variance in *RSD* very well. The erosion-reducing effect of *RD* decreases with increasing *D*. Carrots with very fine roots can reduce soil detachment in a similar way as grass roots. With increasing *D*, the erosion-reducing effect of carrot type roots becomes less pronounced compared to fine roots.

The results indicate a higher erosion-reducing potential of grass roots for silt loam soils compared to sandy loam soils. The erosion-reducing effect of both grass and carrot roots is larger for initially wet soils compared to dry soils, because slaking strongly reduces the effect of increased cohesion provided by roots (De Baets et al. 2007a).

Grasses are as effective in reducing concentrated flow erosion for low as for high flow shear stresses. Carrot roots on the other hand, are less effective in reducing erosion rates when high flow shear stresses are applied. For carrots *RSD* values higher than 1 can be observed, even when tested at a low flow shear stress. When tested at medium and high shear stresses, *RSD* values are often higher for samples with carrot roots compared to grass roots. For carrots growing in a sandy loam soil, significant differences (at the 5 % level) can be observed between shear stress levels, when the root effect is predicted with *RD*. This can be explained by the occurrence of local turbulence and vortex erosion scars around individual carrot roots, which form an obstacle to the flow and increase the detachment rate (De Baets et al. 2007a).

A metadata analysis showed that for fibrous root systems, models using root density and soil moisture information are capable to explain 79 % of the variation in relative erosion rates, whereas relative erosion rates for tap-root permeated topsoils remain difficult to predict with root architectural information only (De Baets and Poesen 2010).

Experimental results also showed that both a random orientation and rows perpendicular to the dominant flow direction are effective in reducing concentrated flow erosion rates by roots. Planting or sowing species in rows parallel to the flow direction does not offer a good protection to erosion by concentrated flow (De Baets et al. 2014).

4.3.2 Field Measurements

Root characteristics of typical Mediterranean plants were measured in the field and an empirical model, linking root characteristics (root density and root diameter) to relative soil detachment rate, was then used to predict the root effect on the resistance to concentrated flow erosion. Plants were sampled in three different habitats, i.e. the ephemeral river channels (Group 1), on abandoned croplands formed in Quaternary loams (Group 2) and in badland areas (semi-natural land consisting of steep incised slopes) formed in marls (Group 3). The root characteristics measured are root:shoot ratio, root density, root diameter and root length density.

The plants are carefully excavated in the field then, after the excavation, digital photos of the root systems are made to describe the root system. Height and diameter of the orthogonal projection of the above ground biomass are measured with a ruler. Then the root system is put on a horizontal plastic sheet (Fig. 4.8) and exposed in the same position as it is growing in the soil and roots are cut into soil depth classes of 10 cm starting for the bottom up to the top of the root system. Roots are collected in a plastic bag per soil depth class and per species. In the laboratory roots from each bag were selected in four diameter classes: <2 mm, 2–5 mm, 5–10 mm, >10 mm. For each diameter class and each depth class root dry mass was assessed. Therefore the roots were put into the oven for 24 h at 60–65 °C (Smit et al. 2000).

Fig. 4.8 Five excavated *Anthyllis* root systems, Cárcavo, Spain (Photo: S. De Baets, January 2005)

Root dry weight per individual and per depth class is then obtained by calculating an average value. Roots from each depth class are also exposed to take digital photographs from which total length was assessed using a digitisation software program (Mapinfo Professional 6.0). For an individual plant species root length per depth class is the average value of the root length of all the plants measured. The total wet above-ground biomass was weighed in total in the field with a field balance. A sample of this biomass was taken to the lab for calculation of moisture content and mean total dry mass of the shoots per individual plant.

To assess the resistance of topsoils reinforced with Mediterranean plant roots to erosion by concentrated flow, the empirical relationships, established for carrots (*Nandor F1 hybride* seeds), weeds (e.g. *Trifolium Repens* L.) and grass (27% of *Lolium perenne*, 21% of *Lolium perenne*, 12% of *Festuca rubra* and 40% of *Festuca arundinacea)* roots during simulated flow experiments in the laboratory on a saturated silt loam soil, were used. These experiments resulted in a negative exponential relationship between relative soil detachment rate (RSD) and RD as a function of root diameter. Different equations could be established to describe the erosion-reducing effect for plant roots of different root diameter classes, whereby the erosion-reducing effect of plant roots decreases with increasing root diameter.

The values of the RSD for the different species within the first 10 cm of topsoil are listed in Table 4.3. This list has been ranked according to the predicted RSD values for the topsoil (0–0.10 m) in order to select species according to their erosion reduction potential. It can be observed that the roots from grasses (family of the *Poaceae*) such as *Helictotrichon filifolium, Piptatherum miliaceum, Juncus acutus, Avenula bromoides, Lygeum spartum* and *Brachypodium retusum* have a very high

Table 4.3 List of species and the potential of their root system for increasing the erosion resistance of topsoils to concentrated flow erosion (De Baets et al. 2007b)

Name of the species	RSD (0–10 cm topsoil)	Erosion reducing Potential
Avenula bromoides	$0.3.10^{-12}$	Very high
Juncus acutus	$2.72\ .10^{-8}$	Very high
Lygeum spartum	$2.41\ .10^{-7}$	Very high
Helictotrichon filifolium	$1.61\ .10^{-6}$	Very high
Plantago albicans	1.10^{-5}	Very high
Brachypodium retusum	8.10^{-4}	Very high
Anthyllis cytisoides	$2.29\ .10^{-3}$	Very high
Piptatherum miliaceum	0.01	Very high
Tamarix canariensis	0.01	Very high
Stipa tenacissima	0.03	High
Retama sphaerocarpa	0.03	High
Salsola genistoides	0.03	High
Artemisia barrelieri	0.07	High
Dorycnium pentaphyllum	0.11	Medium
Rosmarinus officinalis	0.15	Medium
Atriplex halimus	0.18	Medium
Nerium oleander	0.19	Medium
Dittrichia viscosa	0.19	Medium
Fumana thymifolia	0.25	Low
Thymus zygis	0.32	Low
Teucrium capitatum	0.32	Low
Limonium supinum	0.37	Low
Ononis tridentata	0.45	Low
Thymelaea hirsuta	0.5	Very low
Phragmites australis	0.6	Very low
Bromus rubens	0.71	Very low

RSD relative soil detachment rate for the first 10 cm of the topsoil (0 = very high erosion resistance, 1 = very low erosion resistance), 0 < RSD < 0.01 = very high erosion-reducing potential, 0.01 < RSD < 0.10 = high erosion-reducing potential, 0.10 < RSD < 0.25 = medium erosion-reducing potential, 0.25 < RSD < 0.50 = low erosion-reducing potential, RSD > 0.50 = very low erosion-reducing potential

concentrated flow erosion-reducing potential (0 < RSD < 0.01) for the 0–0.10 m thick topsoil. This can be attributed to the high density of fine roots in the topsoil for these species. These grasses only protect the 0–0.20 m thick topsoil. Moreover, comparison of the slope values of the relationship between RSD and soil depth (for the top 0–0.20 m) indicated that the erosion-reducing effect of grasses diminished very rapidly with increasing soil depth compared to the other studied plant species.

4.3.3 Assessment of Stem Density and Trapping Effectiveness

In this study, stem density (SD) was measured for each individual plant species (n = 5 plants per species). The unit area equals the soil surface occupied by the vertical projection of the above-ground biomass and is thus species dependent. The stems were assumed to have a circular cross-section. Stem density for shrubs (SD, $m^2\ m^{-2}$) is calculated as:

$$\text{For Shrubs:} \quad SD = \frac{\sum \pi \left(d_i/2\right)^2}{\pi \left(D_P/2\right)^2} \tag{4.5}$$

where d_i is the diameter of each stem (m) and D_P is the mean diameter of the vertical orthogonal projection of the above-ground biomass (m).

For grasses not all stem diameters were measured separately. Only a representative horizontal area (ca. 5 cm^2) of a section of grasses (S_s, m^2), the corresponding number of stems in this section (n_s) and their mean diameter were measured (d). Additionally the fraction of this area relative to the total surface occupied by vertical projection of the above-ground biomass was assessed to calculate total stem density for grasses (Eq. 4.6).

$$\text{For grasses:} \quad SD = \frac{S_{tot}}{S_s} * \frac{n_s \cdot \pi \left(\frac{d}{2}\right)^2}{S_s} \tag{4.6}$$

where n_s is the number of stems in a horizontal section with area S_s, d is mean stem diameter, S_{tot} (m^2) is the total surface occupied by the vertical projection of the above-ground biomass.

A measure of the sediment and organic debris trapping effectiveness (TE, $m\ m^{-1}$) of plants is the ratio of the diameter (d_i) of the horizontally projected stems on a line perpendicular to the dominant flow direction and the maximum length of this perpendicular line (L_{tot}) defined by the vertical projection of the above-ground biomass, i.e.

$$\text{For shrubs:} \quad TE = \frac{\sum d_i}{L_{tot}} \tag{4.7}$$

where TE is trapping effectiveness, d_i is stem diameter and L_{tot} is the length determined by the projection of the above-ground biomass, in a direction perpendicular to the dominant flow direction (assessed topographically). Bold lines indicate the vertical projection of maximum extent of above-ground biomass. d_i values represent the width of the horizontal projection of all plant stems on L_{tot}.

Stem density (SD) was calculated according to Eqs. 4.5 and 4.6 as a measure for the capacity of plant stems to trap detached sediment and organic residues arriving from different directions. SD ranges from 0.04 to 12.61 %. The two herbs *Plantago albicans* and *Limonium supinum* show the highest stem density measurements. These are small plant species with a good ground cover. Some grasses like *Stipa tenacissima* and *Helictotrichon filifolium* and the studied reeds *Juncus acutus* and *Phragmites australis* also show high stem densities. Other grasses like *Avenula bromoides* and *Lygeum spartum* do not have such high stem densities as expected. This can be explained by the angle of the stems, whereby the total surface under the crown is higher as compared to other grasses.

Trapping effectiveness (TE) of shrubs was measured according to Eq. 4.7 and similarly for herbs and grasses along a line orthogonal to the dominant flow direction, as a measure for the sediment trapping effectiveness assuming that sediment originates from one direction. TE ranges between 3.3 and 35.4 %. The two herbs *Plantago albicans* and *Limonium supinum*, as well as most of the grasses (except *Lygeum spartum*) and the reeds *Juncus acutus* and *Phragmites australis* are shown to be very effective for trapping sediment and organic residues. Also some shrubs like *Rosmarinus officinalis* and *Nerium oleander* have a high obstruction capacity.

More information on stem density and trapping effectiveness values and assessment methods can be found in De Baets et al. (2009).

4.3.4 Laboratory Root Tensile Strength and Stem Bending Tests

Using the same apparatus as used for the tensile strength tests, stem bending tests were also performed to assess modulus of elasticity for individual stems of 25 typical Mediterranean plant species in the laboratory. Root tensile strength (T_r, MPa) tests were conducted in the laboratory with a UTS testing apparatus (Fig. 4.9). The following formula was used to calculate T_r (Bischetti et al. 2005b):

$$T_r = \frac{F_{\max}}{\pi\left(\frac{D^2}{4}\right)} \tag{4.8}$$

where F_{max} is the maximum force (N) needed to break the root and D is the mean root diameter (mm) before stretching.

Modulus of elasticity (E_{mod}) is a material characteristic and can be calculated from the rigidity divided by the second moment of inertia ($I = \pi r^4/4$ for circular stems). For each species, ten samples of 15 cm long stems were tested. Different stem diameters were tested. As reported in many studies (e.g. Bischetti et al. 2005b; Mattia et al. 2005; Norris 2005; Operstein and Frydman 2000; Tosi 2007) root tensile strength (Tr) decreases with increasing root diameter (D), following a power

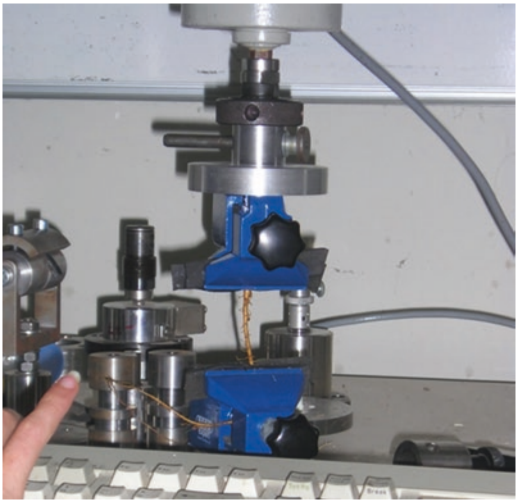

Fig. 4.9 Universal testing System (UTS) apparatus used for root tensile strength measurements at KU Leuven

law equation of the form Y = a X^b. The maximum recorded root tensile strength values amount to 303 mPa for *Nerium oleander* (D = 0.09 mm) and 267.5 mPa for *Tamarix canariensis* (D = 0.1 mm) (De Baets et al. 2008). Root tensile strength values are in the same range of root tensile strength values reported by Bischetti et al. (2005a) for forest species in Northern Italy. Mean root tensile strength does not differ significantly ($p = 0.12$) according to vegetation type (De Baets et al. 2008).

The results from a bending test on the stems show that grasses and fragile shrubs or herbs like *Fumana* and *Limonium* have a high rigidity per unit stem cross-sectional area. The product MEI of stem density (M), modulus of elasticity (E) and moment of inertia (I) combines bending properties with stem density and stem morphology. The results in Table 4.4 show that the shrubs and trees are the most resistant and the grasses and some small shrubs the least resistant to bending simulated under flow shear forces. The reeds show intermediate values.

4.3.5 Synthesis

Based on the various properties measured of the different plant species, a cluster analysis was performed. This analysis resulted in eight clusters, whereby all plants belonging to a cluster show similar performance on the criteria used to select the suitability of species for erosion control (Table 4.5). For more detailed information on the criteria and methods used to select suitable species for rill and gully erosion control reference is made to De Baets et al. (2009).

Table 4.4 MEI values for Mediterranean plant species

Plant name	Vegetation type	MEI (N)
Avenula bromoides	Grass	0.45
Helictotrichon filifolium	Grass	3.62
Fumana thymifolia	Shrub	0.64
Limonium supinum	Herb	0.25
Teucrium capitatum	Shrub	0.62
Lygeum spartum	Grass	0.41
Stipa tenacissima	Grass	0.32
Brachypodium retusum	Grass	0.05
Artemisia barrelieri	Shrub	2.70
Piptatherum miliaceum	Grass	2.09
Juncus acutus	Reed	1.77
Dittrichia viscosa	Shrub	13.58
Dorycnium pentaphyllum	Shrub	22.27
Phragmites australis	Reed	5.54
Anthyllis cytisoides	Shrub	8.56
Thymelaea hirsuta	Shrub	17.04
Atriplex halimus	Shrub	54.16
Thymus zygis	Shrub	11.96
Tamarix canariensis	Tree	48.48
Nerium oleander	Shrub	25.17
Rosmarinus officinalis	Shrub	159.80
Salsola genistoides	Shrub	42.17
Retama sphaerocarpa	Shrub	27.51
Ononis tridentata	Shrub	97.54

4.4 Effects of Vegetation in Channels

4.4.1 Roughness and Hydraulics

Determining the effect that different plant assemblages have on flow hydraulics is key to evaluating the potential for vegetation to withstand erosive forces of floods, increase the overall resistance of the channel to erosion and reduce the connectivity of sediments along river channels. In order to calculate hydraulics surveyed cross-sections and estimated Manning's n values for specified flow stages are entered as input into software package WinXSPRO (Hardy et al. 2005) and the velocity and discharge is computed. The output generated by WinXSPRO can then be used to calculate other hydraulic values such as unit power, shear stress and shear velocity. The advantage of WinXSPRO is that the cross-sections can be divided into subsections and different Manning's n values applied (Sandercock and Hooke 2010). Thus differentiation due to different zones of vegetation can be incorporated. The values of n were assigned according to guidelines in Arcement and Schneider (1989).

Table 4.5 Plant species grouped in eight clusters according to their scoring for the four main requirements, i.e. (1) the potential to prevent incision by concentrated flow erosion, (2) the potential to improve slope stability, (3) the potential to resist bending by water flow and (4) the ability to trap sediments and organic debris (De Baets et al. 2009 Earth Surface Processes and Landforms 34: 1374–1392)

Cluster	Plant species name	Cluster description
1	*Fumana thymifolia* *Teucrium capitatum*	low resistance to erosion, low trapping effectiveness, not resistant to removal, no potential to improve slope stability
2	*Nerium oleander* *Rosmarinus officinalis*	low potential for slope stabilisation medium potential to prevent erosion by concentrated runoff high resistance to bending, medium trapping effectiveness
3	*Anthyllis cytisoides* *Retama sphaerocarpa* *Salsola genistoides* *Tamarix canariensis* *Atriplex halimus*	high potential for slope stabilization, very resistant to removal, low trapping effectiveness and medium to high potential to prevent concentrated flow erosion
4	*Thymus zygis* *Artemisia barrelieri* *Lygeum spartum* *Avenula bromoides* *Piptatherum miliaceum*	medium to high potential to prevent erosion, low potential for slope stabilisation medium trapping effectiveness and low resistance to removal
5	*Stipa tenacissima* *Thymelaea hirsuta* *Dittrichia viscosa* *Ononis tridentata* *Dorycnum pentaphyllum*	medium potential for slope stabilisation, low potential to prevent incision medium to high resistance to removal, low trapping effectiveness
6	*Plantago albicans* *Limonium supinum* *Helictotrichon filifolium* *Brachypodium retusum*	medium to high potential to prevent concentrated flow erosion, easy to remove low potential for slope stabilization and high trapping effectiveness
7	*Juncus acutus*	high potential to prevent erosion, high trapping effectiveness and medium resistant to removal
8	*Phragmites australis*	medium resistant to removal, high trapping effectiveness, medium to low potential to prevent erosion

Tables of component Manning's n values have been compiled based on extensive work on channels in Arizona where roughness values have been measured (Aldridge and Garrett 1973; Arcement and Schneider 1989) and verified (see O'Day and Phillips 2000; Phillips and Hjalmarson 1994; Phillips and Ingersoll 1998; Phillips et al. 1998), and which have similarities to those which are being studied in Southeast Spain. The hydraulics of flows have been calculated at selected sites for minor, moderate and high discharge events along two channels in Southeast Spain, Cárcavo (2, 10 and 40 $m^3 s^{-1}$) and Torrealvilla (10, 100 and 200 $m^3 s^{-1}$). These discharges were selected as having ecological and geomorphological significance. The low flow fills the thalweg/inner channel, the medium flood most closely resembles that

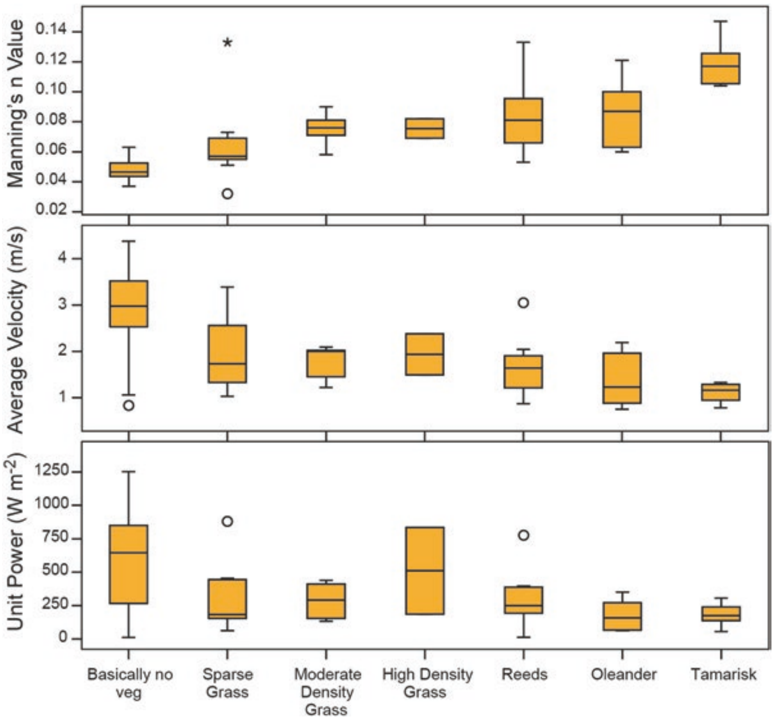

Fig. 4.10 Output from hydraulic computations for high flow (40 m^3 s^{-1}) along Cárcavo showing the influence that Manning's n value for different vegetation types has on average velocity and unit power (After Sandercock and Hooke 2010)

of a bankfull and the high flow is at least twice the magnitude of the medium flow. Very sparse information is published or available on the frequency and magnitude of flows but monitoring of flows within the Guadalentín Basin over the previous 10 years also informed selection of these flows (Hooke 2007a).

As is to be expected, as Manning's n values increase there is a reduction in the velocity and unit power of flows, this reflecting in part the effect that vegetation has in increasing the roughness of the channel. This is demonstrated most clearly in Figs. 4.10 and 4.11 which show the output of the hydraulic computations for the high flood at Cárcavo and Torrealvilla sites respectively. Highest velocities are associated with grasses which have low Manning's n values (they are also positioned low in the channel). Comparably lower velocities are also associated with Oleander and Tamarisk, this attributed to the high Manning' n values but also their tendency to establish on more elevated surfaces. Reeds are also associated with lower flow velocities, this in part is a function of the very low gradients where these plants establish.

To assess the resistance of different plants to erosion, these models need to be informed by field surveys, where flood effects on vegetation have been documented.

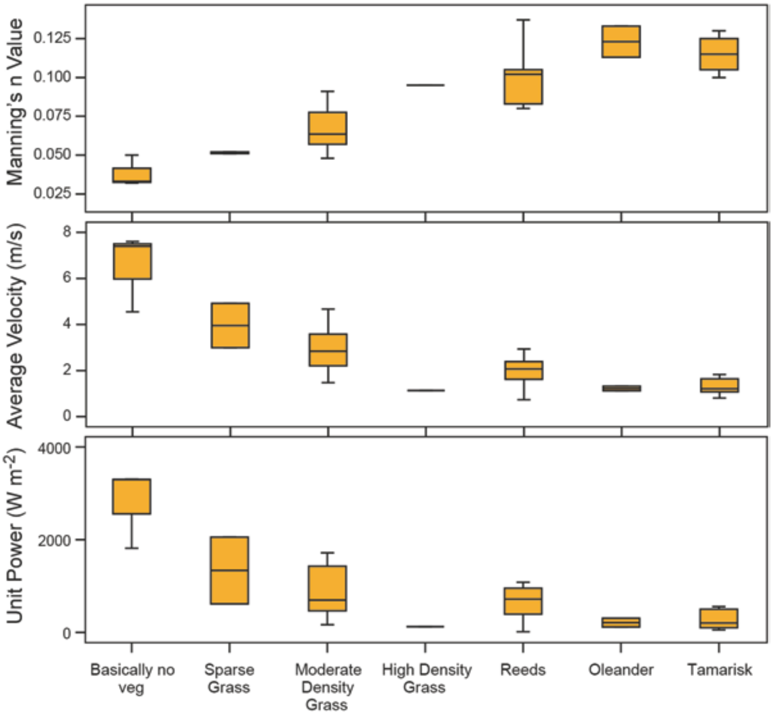

Fig. 4.11 Output of hydraulic computations for high flow (200 $m^3 s^{-1}$) along Torrealvilla showing influence that Manning's n value has on average velocity and unit power (After Sandercock and Hooke 2010)

For this, we drew upon the impact that floods in September 1997 (Hooke and Mant 2000) and October 2003 within the Guadalentín Basin (Salada) and November 2006 in Cárcavo have had on vegetation and channel morphology. The hydraulics of floods and forces acting on vegetation were calculated using detailed cross-sections and flood debris lines. The effects of these floods on vegetation provide the basis for assessing the thresholds of forces for plant damage and destruction. This information can then be fed back into the models, to predict what would be the likely response of the vegetation and channel morphology to a particular flood. The results in relation to a range of species found in the channels and on floodplains are presented in Fig. 4.12, documenting cases where vegetation suffered no change, battered, swept over, flattened, mortality or removed in relation to calculated shear stress and velocity values. Instances of mortality or removal of vegetation are rare, though some data do exist.

Of the two dominant species of grasses that are found in these channels, *Piptatherum miliaceum* and *Lygeum spartum*, the latter demonstrates greater resistance to flows. *Piptatherum miliaceum* are swept over and flattened by flows with shear stresses of <200 N m^{-2} and velocities of 1.7 m s^{-1}. Some cases of removal

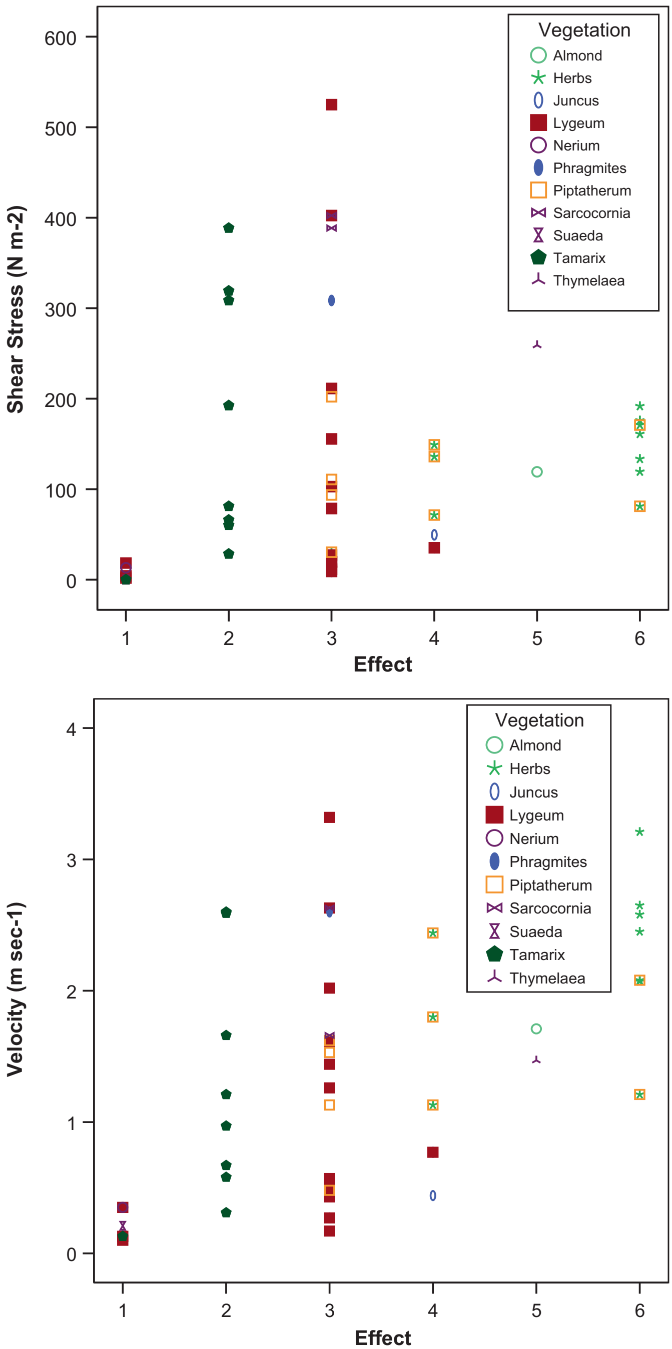

Fig. 4.12 Summary of effects on vegetation for flows in Torrealvilla (September 1997), Salada (November 2004) and Cárcavo (November 2006) in relation to calculated shear stresses and velocity. 1 = no change, 2 = battered, 3 = swept over, 4 = flattened, 5 = mortality, 6 = removed

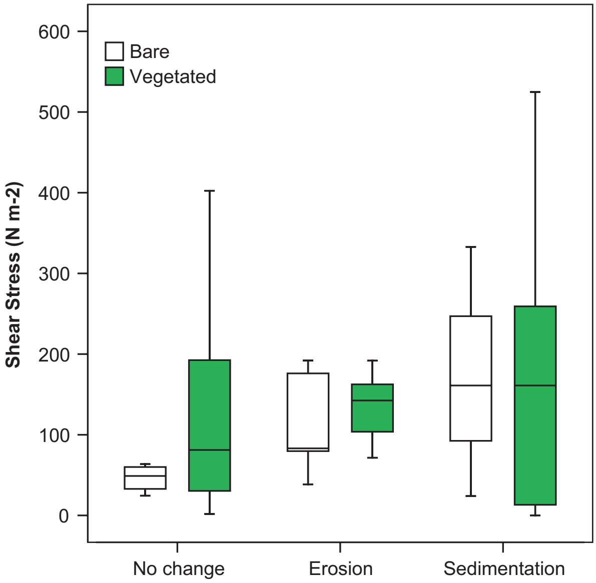

Fig. 4.13 Processes in bare and vegetated patches in relation to shear stresses of flow

were also documented for flows with shear stresses of 90 and 180 N m^{-2} (Velocity 1.2 and 2.1 m s^{-1}). No instances of removal of *Lygeum spartum* were documented for the flows studied, the plants being swept over or flattened. Herbs were flattened by flows with shear stresses of 70–160 N m^{-2} (velocity 1–2.5 m s^{-1}) and removed by flows with shear stresses of 90–200 N m^{-2} (1.2–3.2 m s^{-1}).

Aerial parts of *Juncus* (species *Juncus maritimus*), also have a low resistance to erosion: these were flattened by flows with shear stresses < 50 N m^{-2} and velocities < 0.5 m s^{-1} (but no instances of removal recorded). In comparison, *Phragmites australis* has a higher resistance to erosion with flattening by flow of 300 N m^{-2} (no erosion occurred with this flow as reeds formed a mat on surface). Flattening and mortality of the shrub *Thymelaea hirsuta* occurred in response to the high flow event on Salada; the flow affecting the vegetation had shear stresses of 250 N m^{-2} and velocity of 1.5 m s^{-1}. Insufficient data exists on *Nerium oleander*, but indications are that it is highly resistant to flows. They were very battered at Oliva site along the Torrealvilla in 1997 but have since resprouted. *Tamarix canariensis* also has a very high resistance to flows. These species were battered by flows up to 400 N m^{-2} with velocities of 2.7 m s^{-1} along Salada, but no incidences of flattening or removal have been encountered (except for some small individuals, not calculated here), though they can be bent. Some poplar trees were snapped off in the 1997 flood at Oliva. A number of instances where Almond trees have been affected by floods has been documented, one case of mortality presented here, was a result of a flow with shear stress of 120 N m^{-2} and velocity of 1.7 m s^{-1}.

Figure 4.13 presents an analysis of bare and vegetated areas within channels, showing the range of forces for each where there was no change, erosion and sedimentation. The effect of vegetation in increasing the resistance of the channel to erosion is clear when comparing the distribution of forces for vegetated patches against bare patches. Within vegetated patches, flows up to 400 N m^{-2} with velocities of 3.2 m s^{-1} were not capable of causing erosion, whilst bare areas had a much lower upper limit of flows which caused erosion (shear stresses < 70 N m^{-2} and velocities < 1.7 m s^{-1}).

Minor floods have relatively little impact on vegetation and channel form, patches of reeds may be swept over, with some minor incision being restricted to the thalweg (such as the November 2006 event). The overall impact of this flood is positive, contributing water to growth of plants and refilling local aquifers. A moderate flood (such as the September 1997 event) results in greater incision and widening of the channel and exceeds the threshold for the removal of herbs, and battering of vegetation. These events have a negative impact on vegetation, however, recovery can be fairly rapid. A major flood (such as the October 2003 event) is likely to cause significant morphological changes, removal of herbs and flattening of vegetation. An extreme flood, such as that which occurred in the region in October 1973 and in September 2012 with flow depths up to 5 m is likely to cause major channel adjustments, with erosion and widening of the channel, massive scour and headcut formation and extension. All vegetation may be removed, although *T. canariensis* may withstand such an event. Subsequent events may have greater geomorphological effect due to the degraded condition of the channel.

4.5 Summary

Studying the effect plants have on processes has been a major component of the project and these have been reported on in this chapter.

A climatic threshold for cover crops was identified, based on the relation between tree density, projected canopy cover and climate. As a climatic indicator the Humidity Index (*HI*) which is the ratio between annual precipitation and evapotranspiration was used. For locations where $HI > 0.6$, the growth of olive trees is no longer limited by water availability and there is a surplus of water that could be used to grow cover crops. Below this threshold, the use of cover crops must be restricted in space and time to avoid competition for water. Field surveys of roots showed that deep rooted almond crops and shallow rooted cover crops derive their water from different parts of the soil. The results of further modelling of water balance in the plough layer showed that more water is available for cover crops in orchards on marly soils than in orchards on stony soils, the difference being related to the deeper infiltration of rain on the stony soils. The results of this work indicate that there are opportunities for applying cover crops without a negative effect on the growth and yield of the tree crop. In addition, results from water budget modelling for one almond field in Cárcavo indicated that there was greater water availability for cover crops in depressions.

Vegetation has a significant influence on hydrological pathways as shown in the work on semi-natural and abandoned lands. As vegetation develops it modifies pathways of water and sediments, with higher infiltration under vegetation patches and sedimentation behind vegetation. Water repellency also plays an important role in the local redistribution of water over soils: accumulated organic matter and water repellency may increase runoff and generate unwanted connectivity. The formation of soil crusts in bare areas after land abandonment also reduces the infiltration capacity of the soil resulting in increases in runoff and erosion.

A large amount of data has been collected on the above and below ground attributes of plants that are important in reducing erosion, From the various experiments and field measurements, both root and shoot properties have then been combined to assess the suitability of plants for erosional control in three different areas prone to water erosion: channels, abandoned croplands and steep badland slopes. Grasses like *Helictotrichon filifolium*, *Piptatherum miliaceum*, *Avenula bromoides*, *Lygeum spartum* and *Brachypodium retusum* have the highest potential to reduce soil erosion rates, but shrubs such as *Anthyllis cytisoides* and the tree *Tamarix canariensis* are also effective in reducing erosion rates. Within channels *Juncus acutus* and *Tamarix canariensis* have the highest potential to reduce erosion. *Salsola genistoides* is the most suitable species to control gully erosion on steep slopes, but also the grasses *Helictotrichon filifolium* and *Stipa tenacissima* can be planted to increase the resistance to erosion. On Abandoned fields, *Rosmarinus* and *Plantago albicans* are the most effective species in reducing concentrated flow erosion rates.

From measurements of plant properties and of effects of flows in channels, effectiveness of plants to reduce erosion and increase sedimentation in channels has been assessed. Grasses such as *Lygeum spartum*, the shrub species *Nerium oleander* and Tree species *Tamarix canariensis* are found to be highly resistant to removal. Of particular interest is *Lygeum spartum*, having an affinity for fine sediments, and its ability to trap further fines and form vegetated mounds. Spatial comparisons show that the effect vegetation has in trapping sediments is dependent on its location in the channel network.